

# Low Speed Control of an Autonomous Vehicle Using a Hybrid Fractional Order Controller

S. Hassan HosseinNia, Inés Tejado, Blas M. Vinagre, Vicente Milanés, Jorge Villagrà

**Abstract**—Highly non-linear vehicle dynamics plays an important role in autonomous driving systems, especially in congested traffic situations at very low speeds. Due to this fact, accurate controllers are needed in order to ensure safety during navigation. In this paper, based on a previous fractional order speed control, an improved fractional order control is presented to control a commercial Citroën C3 prototype –which has automatic driving capabilities– at low speeds, which considers a hybrid model of the vehicle. Specifically, two different fractional order  $PI^\alpha$  controllers are designed to act over the throttle and brake pedals, respectively. Concerning to the uncertain dynamics of the system during the brake action parameters are tuned to design a robust controller. In addition, the system is modeled as hybrid fractional order differential inclusions. Experimental and simulation results, obtained in a real circuit, are given to demonstrate the effectiveness of the proposed strategies for cruise control at low speeds.

## I. INTRODUCTION

Research on traffic safety is continuously developing and carried out around the world. In particular, the aim is to develop active systems, called advanced driver assistance systems (ADAS), which will be able to prevent accidents (see [1]). One of the systems included in commercial vehicles to increase safety in carrying out driving-related tasks is cruise control (CC). Standard cruise control (CC) will automatically adjust the vehicle speed regarding to the desired reference velocity. Automotive sector has included in its commercial vehicles some advances for driving in urban areas. From the efficiency point of view, the Start&Stop system in [2] permits switching off the vehicle's engine when it is stopped because of traffic lights or jams. Therefore,  $CO_2$  emissions are significantly reduced. Nevertheless, from the safety point of view, autonomous systems capable of aiding the driver in case of congested traffic situations still remain as an unsolved problem. The main difficulty arises from the highly non-linear dynamics of vehicles at very low speeds.

Fractional order control (FOC), that is, the generalization to non-integer orders of traditional controllers or control schemes, and its applications are becoming an important issue since it translates into more tuning parameters or, in

other words, more adjustable time and frequency responses of the control system, allowing the fulfillment of robust performances. It has been applied, in a satisfactory way, in several automatic control applications (see [3], [4] and references therein) leading to the conclusion that FOC is preferred to other techniques (the better performance of this type of controllers, in comparison with the classical PID ones, has been demonstrated e.g. in [5] and [6]). However, FOC has not been applied to low speed control of autonomous vehicles, expecting robust results.

With the above motivation, this paper deals with the design and implementation of the CC of the commercial Citroën C3 vehicle is addressed. As a matter of fact, based on a hybrid model of the vehicle, which considers different models for vehicle dynamics when accelerating and braking, two fractional order  $PI^\alpha$  controllers are designed for CC manoeuvres at low speeds. Moreover, the system will be modeled by fractional order hybrid differential inclusions.

The rest of the paper is organized as follows. Section II briefly describes the modifications performed in the vehicle to act autonomously on the throttle and brake pedals, as well as the dynamic longitudinal model obtained for this kind of manoeuvres. Section III addresses the fractional order CC of the vehicle acting over the throttle and brake pedals. Simulation and experimental results are given in Section IV to validate the proposed CC. Finally, concluding remarks are included in Section V.

## II. AUTOMATIC VEHICLE

To design the cruise control manoeuvres at very low speeds, a model of the automatic vehicle –a commercial convertible Citroën C3 Pluriel (see Fig. 1)– was obtained experimentally, which includes its dynamics when accelerating and braking at very low speeds. This section briefly describes the modifications performed in the vehicle to act autonomously on the throttle and brake pedals, as well as its dynamic longitudinal model.

### A. Description

The vehicle control system for automatic driving follows the classical perception-reasoning-action paradigm [7],[8]. The first stage is in charge of localizing as precisely and robustly as possible the vehicle. To that end, the following subsystems are embedded in the vehicle

- A double-frequency global positioning system (GPS) receiver running in real-time kinematic (RTK) carrier phase differential mode that supplies 2cm of resolution positioning at a refresh rate of 5Hz.

This work has been partially supported by research grants TRA2008-06602-C01 and TRA2008-06602-C02 (Spanish Ministry of Science and Innovation).

S. Hassan HosseinNia, Inés Tejado and Blas M. Vinagre are with Dept. of Electrical, Electronic and Automation Engineering, Industrial Engineering School, University of Extremadura, Badajoz, Spain. (email: {hoseinnia,itejbal,bvinagre}@unex.es)

Vicente Milanés, Jorge Villagrà are with the AUTOPIA Program at the Centre for Automation and Robotics (CAR, UPM-CSIC), Ctra. Campo Real km 0.22, La Poveda-Arganda del Rey, 28500 Madrid, Spain. (e-mail: {vicente.milanes,jorge.villagra}@csic.es)



Fig. 1: Experimental vehicle

- A wireless local area network (IEEE 802.11) support, which allows the GPS to receive both positioning error corrections from the GPS base station and vehicle and positioning information from the preceding vehicle.
- An inertial measurement unit (IMU) Crossbow IMU 300CC placed close to the centre of the vehicle to provide positioning information during GPS outages.
- Car odometry supplied by a set of built-in sensors in the wheels, whose measurements can be read by accessing the controller area network (CAN) bus of the vehicle. This is implemented by means of a CAN Card 2.6.

Thereafter, an on-board computer is in charge of requesting values from each of the on-board sensors with which to compute the controller's input values. Finally, the devices that make possible to act on the throttle and brake of the car are an electrohydraulic system capable of injecting pressure into the car's anti-block braking system (ABS), and an analogue card which can send a signal to the car's internal engine computer to demand acceleration or deceleration. The electro-hydraulic braking system is mounted in parallel with the original one. Two shuttle valves are installed connected to the input of the anti-lock braking system (ABS) in order to keep the two circuits independent. A pressure limiter tube set at 120bars is installed in the system to avoid damage to the circuits. Two more valves are installed to control the system: a voltage-controlled electro-proportional pilot to regulate the applied pressure, and a spool directional valve to control the activation of the electrohydraulic system by means of a digital signal. These two valves are controlled via an I/O digital-analogue CAN card. The voltage for the applied pressure is limited to 4V (greater values correspond to hard braking and are not considered).

### B. Dynamic longitudinal model

Due to the impossibility of obtaining the exact dynamics that describes the vehicle, in this work the idea is to obtain a simple linear model of the vehicle for the circuit wherein the experimental manoeuvres will be performed.

The vehicle longitudinal dynamics can be simplified by a first order transfer function [9] that relies the vehicle velocity and a proportional voltage to the throttle angle:

$$G(s) \simeq \frac{K}{s+p} = \frac{4.39}{s+0.1746}, \quad (1)$$

Simple linear longitudinal models have been also used in [10] and [11]. The reason why there is no need to use a

more complex model arises from the kind of manoeuvres we perform in this work, as will be stated from the experimental results.

Besides, vehicle dynamics in braking maneuvers can be given by an uncertain first order transfer function that depends on the voltage applied to the brake pedal [12].

$$G(s) \simeq \frac{1}{\tau s + 1}, \quad (2)$$

where the time constant  $\tau$  varies with the action over the brake in the interval  $\tau \in [1.6, 3.1]$ s.

### III. CRUISE CONTROL

This section presents a hybrid CC of the vehicle at low speeds based on the different vehicle's dynamics when accelerating and braking. In particular, the fractional order  $PI^\alpha$  controller designed in [9] will be used for the throttle action –it was designed to control the throttle and brake pedals, but neglecting the dynamics during braking–, whereas the brake will be controlled by a robust fractional order PI due to the system uncertainty described previously. The motivation of improving that design by considering a hybrid model of the vehicle mainly arises from its application to ACC manoeuvres, in which the adequate control of the brake pedal plays a key role for the success of the whole test. Some considerations on the switching of the controllers are also included.

The most important mechanical and practical requirement of the vehicle to take into account during the design process is to obtain a smooth vehicle's response so as to guarantee its acceleration to be less than the well-known comfort acceleration, i.e. less than  $2m/s^2$ . It must be also mentioned that both velocity and brake control inputs are normalized to the interval  $[-1, 1]$ , where positive values mean throttle actions and the negative, brake ones.

#### A. Throttle Control

In previous works, some traditional PI controllers have been designed (refer e.g. to [14]), and in [9] a fractional order PI controller was proposed. A fractional order PI controller can be represented as follows:

$$C(s) = k_{p1} + \frac{k_i}{s^\alpha} = k_{p1} \left( 1 + \frac{z_c}{s^\alpha} \right), \quad \text{with } z_c = k_i/k_{p1}. \quad (3)$$

Let assume that the gain crossover frequency is given by  $\omega_c$ , the phase margin is specified by  $\varphi_m$  and the output disturbance rejection is defined by a desired value of a sensitivity function  $S(s)$  for a desired frequencies range. For meeting the system stability and robustness, the three specifications to fulfill are the following:

1. Phase margin specification:

$$\text{Arg}[G_{ol}(j\omega_{cp})] = \text{Arg}[C(j\omega_{cp})G(j\omega_{cp})] = -\pi + \varphi_m. \quad (4)$$

2. Gain crossover frequency specification:

$$|G_{ol}(j\omega_{cp})| = |C(j\omega_{cp})G(j\omega_{cp})| = 1. \quad (5)$$

3. Output disturbance rejection for  $\omega \leq \omega_s = 0.035\text{rad/s}$ :

$$|S(j\omega)|_{dB} = \left| \frac{1}{1 + C(j\omega)G(j\omega)} \right|_{dB} \leq -20\text{dB}, \quad \omega \leq \omega_s. \quad (6)$$

Using these three specification and solving the following equations the controller parameters will be obtained [9].

$$z_c = \frac{-\tan \left[ \arctan \left( \frac{\omega_{cp}}{p} \right) + \phi_m \right]}{\omega_{cp}^{-\alpha} \left\{ \sin \phi + \cos \phi \tan \left[ \arctan \left( \frac{\omega_{cp}}{p} \right) + \phi_m \right] \right\}}. \quad (7)$$

$$\frac{Kk_{p1} \sqrt{(1 + z_c \omega_{cp}^{-\alpha} \cos \phi)^2 + (z_c \omega_{cp}^{-\alpha} \sin \phi)^2}}{\sqrt{\omega_{cp}^2 + p^2}} = 1$$

$$k_{p1}^2 + k_i^2 \omega_{cp}^{-2\alpha} + 2k_{p1}k_i \omega_{cp}^{-\alpha} \cos \phi = \frac{\omega_{cp}^2 + p^2}{K^2}. \quad (8)$$

$$|S| = \left| \frac{1}{1 + k_{p1} [1 + z_c \omega^{-\alpha} \cos \phi - jz_c \omega^{-\alpha} \sin \phi] \left( \frac{K}{j\omega + p} \right)} \right|. \quad (9)$$

Solving the set of equations (7), (8) and (9) with the Matlab function *fsolve*, the values of the controller parameters are:  $k_{p1} = 0.09$ ,  $k_i = 0.025$  and  $\alpha = 0.8$ .

### B. Brake Control

As shown, when the brake is active, vehicle dynamics is different, so the brake pedal needs its own controller. In particular, in order to have a robust controller for the uncertain model identified in (2), a robust fractional order PI controller is designed based on the method proposed in [13]. For the purpose of robustness to time constant variations, the gain and phase margins have been also taken as the main indicators. Thus, the specifications to meet are the ones in (4) and (5), referred to phase margin ( $\phi_m$ ) and phase crossover frequency ( $\omega_{cp}$ ) specifications, and the one referring to gain margin ( $M_g$ ), i.e.:

$$\text{Arg}(C(j\omega_{cg})G(j\omega_{cg})) = -\pi, \quad (10)$$

$$\left| C(j\omega_{cg})G(j\omega_{cg}) \right|_{dB} = 1/M_g, \quad (11)$$

where  $\omega_{cg}$  is the gain crossover frequency. Replacing (2) and (3) in equations (4), (5), (10) and (11), brake specifications can be given by the following set of four nonlinear equations

with the four unknown variables ( $k_{p1}, k_i, \alpha, \omega_{cg}$ ):

$$\arctan \left( \frac{k_{p1} \omega_{cp}^{\alpha} \sin \frac{\alpha\pi}{2}}{k_i + k_{p1} \omega_{cp}^{\alpha} \cos \frac{\alpha\pi}{2}} \right) - \arctan(\tau \omega_{cp}) + \frac{(2-\alpha)\pi}{2} - \phi_m = 0, \quad (12)$$

$$\arctan \left( \frac{k_{p1} \omega_{cg}^{\alpha} \sin \frac{\alpha\pi}{2}}{k_i + k_{p1} \omega_{cg}^{\alpha} \cos \frac{\alpha\pi}{2}} \right) - \arctan(\tau \omega_{cg}) + \frac{(2-\alpha)\pi}{2} = 0, \quad (13)$$

$$20 \log \left( \frac{\sqrt{(k_i + k_{p1} \omega_{cp}^{\alpha} \cos \frac{\alpha\pi}{2})^2 + (k_{p1} \omega_{cp}^{\alpha} \sin \frac{\alpha\pi}{2})^2}}{\omega_{cp}^{\alpha} \sqrt{(\tau \omega_{cp})^2 + 1}} \right) = 0, \quad (14)$$

$$20 \log \left( \frac{\sqrt{(k_i + k_{p1} \omega_{cg}^{\alpha} \cos \frac{\alpha\pi}{2})^2 + (k_{p1} \omega_{cg}^{\alpha} \sin \frac{\alpha\pi}{2})^2}}{\omega_{cg}^{\alpha} \sqrt{(\tau \omega_{cg})^2 + 1}} \right) - \frac{1}{M_g} = 0. \quad (15)$$

To reach out its solution, the Matlab function *FMINCON* was used, which finds the constrained minimum of a function of several variables. In this case, (14) was considered as the main function whose parameters are optimized taking into account (12), (13) and (15) as its constraints and setting  $\phi_m$ ,  $\omega_{cp}$  and  $M_g$  to 90deg, 0.3rad/s and 4, respectively. Thus, the obtained controller parameters are:  $k_{p1} = 0.07$ ,  $k_i = 0.11$  and  $\alpha = 0.45$ .

Fig. 2 shows the Bode plots of the controlled system by applying the designed controller. As it can be observed, the cross over frequency is  $\omega_{cp} = 0.7\text{rad/s}$  and the phase margin is  $\phi_m = 93\text{deg}$ , fulfilling the design specifications. Moreover, the system is robust to the time constant variation, which is also fulfilled as illustrated in Fig. 3.

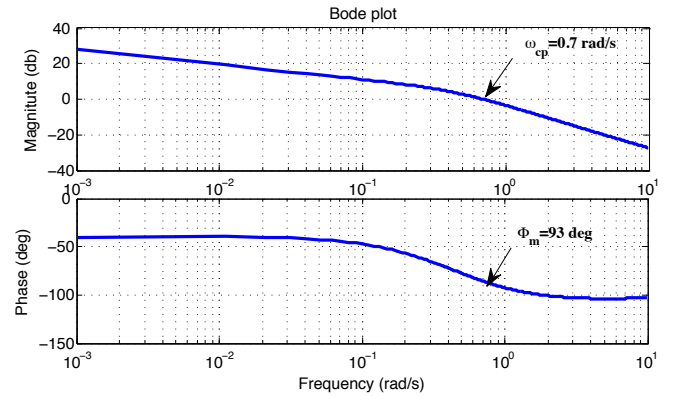


Fig. 2: Bode plots of the controlled vehicle by applying the designed PI $^{\alpha}$  brake controller

Table I summarizes the parameters of the controllers for brake and throttle control.

### C. Hybrid Modeling of the Controlled System

As mentioned before, velocity are controlled with fractional order PI in both brake and throttle actions. Regarding to throttle and brake dynamics, consider a first order system

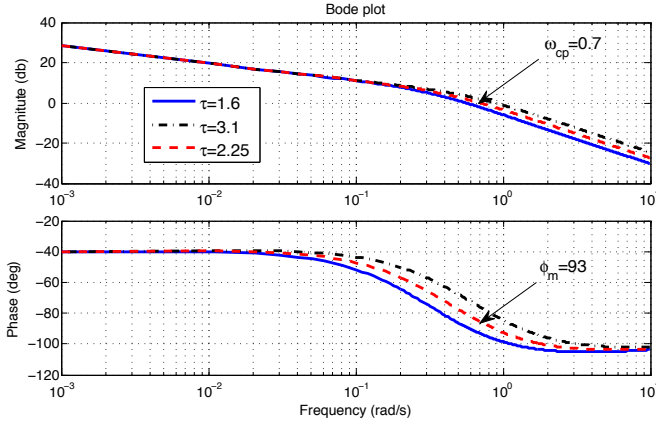


Fig. 3: Comparison of Bode plots of the controlled vehicle by applying the designed  $PI^\alpha$  brake controller with different values of  $\tau$

TABLE I: Parameters of the  $PI^\alpha$  controller for CC

Controller for	$k_{p1}$	$k_i$	$\alpha$
Throttle	0.09	0.025	0.8
Brake	0.07	0.11	0.45

with two different dynamics as follows:

$$G_i(s) = \frac{K_i}{s + \tau_i}, i = 1, 2, \quad (16)$$

Now consider following fractional order PI to control this system,

$$C_i(s) = k_{p_i} + \frac{k_{i_i}}{s^{\alpha_i}}, i = 1, 2. \quad (17)$$

where the the parameters regarding to throttle and brake dynamics are shown in following table:

TABLE II: Parameters of the system and controller in throttle and brake action

	$k_{p1_i}$	$k_{i_i}$	$\alpha_i$	$K_i$	$\tau_i$
Throttle ( $i = 1$ )	0.09	0.025	0.8	4.39	0.1746
Brake ( $i = 2$ )	0.07	0.11	0.45	$\frac{1}{\tau}$	$\frac{1}{\tau}$

where  $\tau \in [1.6, 3.1]$ , concerning to the brake action. Closed loop transfer function of the system can be represent as,

$$\frac{Y(s)}{R(s)} = \frac{a_i s^{\alpha_i} + b_i}{s^{\alpha_i+1} + (\tau_i + a_i) s^{\alpha_i} + b_i}, i = 1, 2. \quad (18)$$

where  $a_i = K_i k_{p1_i}$  and  $b_i = K_i k_{i_i}$ . Assuming  $\alpha_i = \frac{p_i}{q_i}$ , (18) can be represented as state space:

$$\begin{aligned} D^{\frac{1}{q_i}} x &= \mathcal{A}_i x + \mathcal{B}_i r(t), \\ y &= \mathcal{C}_i x. \end{aligned} \quad (19)$$

where  $x = [x_1 \ x_2 \ \dots \ x_{p_i+1} \ \dots \ x_{p_i+q_i-1} \ x_{p_i+q_i}]^T$ ,  
 $\mathcal{A}_i = \begin{bmatrix} 0 & 1 & 0 & \dots & 0 & \dots & 0 \\ 0 & 0 & 1 & \dots & 0 & \dots & 0 \\ \vdots & \vdots & \vdots & \ddots & \vdots & \ddots & \vdots \\ 0 & 0 & 0 & \dots & 1 & \dots & 0 \\ \vdots & \vdots & \vdots & \ddots & \vdots & \ddots & \vdots \\ 0 & 0 & 0 & \dots & 0 & \dots & 1 \\ -b_i & 0 & 0 & \dots & -(\tau_i + a_i) & \dots & 0 \end{bmatrix}$ ,  $\mathcal{B}_i = \begin{bmatrix} 0 \\ 0 \\ 0 \\ \vdots \\ 0 \\ \vdots \\ 1 \end{bmatrix}$ ,  
and  $\mathcal{C}_i = [b_i \ 0 \ \dots \ a_i \ \dots \ 0 \ 0]$ . Now assume that the controller one i.e.  $c_1(e)$  will be activated if  $e = r(t) - y(t) > -\varepsilon$ , ( $r(t) = V_{ref}(t)$  and  $y(t) = V(t)$ ) and the other controller i.e.  $c_2(e)$  will be activated if  $e = r(t) - y(t) < \varepsilon$ . Thus, the flow set and the flow map are taken to be,

$$D^{\frac{1}{q_i}} \begin{bmatrix} x \\ i \end{bmatrix} = \begin{bmatrix} \mathcal{A}_i x + \mathcal{B}_i r_i(t) \\ 0 \end{bmatrix}, \quad (20)$$

$$\begin{aligned} C := \{ (x, i) \in \mathbb{R}^{\alpha_i+1} \times \{1, 2\} \mid & i = 1 \ \& \\ & y(t) < r(t) + \varepsilon \ \text{or} \ i = 2 \ \& \\ & y(t) > r(t) - \varepsilon \}. \end{aligned} \quad (21)$$

The jump set is taken to be:

$$\begin{aligned} D := \{ (x, i) \in \mathbb{R}^{\alpha_i+1} \times \{1, 2\} \mid & i = 1 \ \& \\ & y(t) = r(t) + \varepsilon \ \text{or} \ i = 2 \ \& \\ & y(t) = r(t) - \varepsilon \}. \end{aligned} \quad (22)$$

Regarding the jump map, since the role of jump changes is to toggle the logic mode and since the state component  $x$  does not change during jumps, the jump map will be

$$\begin{bmatrix} x \\ i \end{bmatrix}^+ = \begin{bmatrix} x \\ 3 - i \end{bmatrix}. \quad (23)$$

Fig. 4 shows the switching between throttle and brake action corresponding to the  $\varepsilon = 0$ . It is obvious that the systems is stable during switching of throttle or brake action.  $S_1$  represent the region where the throttle is active and  $S_2$  shows the region where the brake is active.

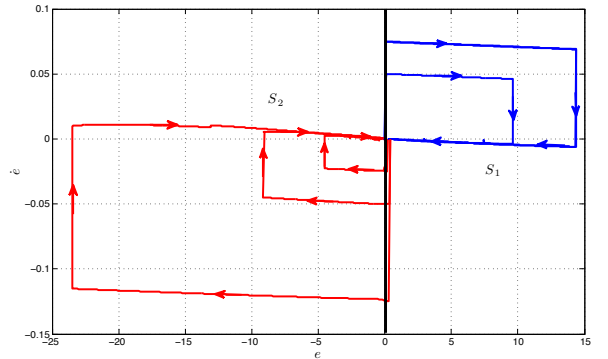


Fig. 4: Switching phases

#### IV. EXPERIMENTAL AND SIMULATION RESULTS

The designed controllers have been tested in simulation and on the real vehicle in the CAR's private driving circuit illustrated in Fig. 5. This circuit has been designed with scientific purposes so only experimental vehicles are driven in this area. It includes 90deg bends and different slopes so as to validate the controller in different circumstances as close to a real environment as possible.



Fig. 5: Private driving circuit at the Center for Automation and Robotics

The simulation results are carried out in the MATLAB/Simulink environment. In order to show the efficiency of the robust controller, a random noise with mean value of 0.85 is added to nominal value of  $\tau = 2.25$ . To show the brake action and the performance of the robust controller which is designed for uncertain system (2), the car moved with fixed pedal to reach the velocity of 30km/h; then, the brake controller is activated. The experimental brake results are shown in Fig. 6. As aforementioned, the main important limitation which have been considered is acceleration i.e.  $[-2, 2]$ . Regarding to this results it is obvious that the application of the robust fractional order controller fulfills the acceleration limitation for the system.

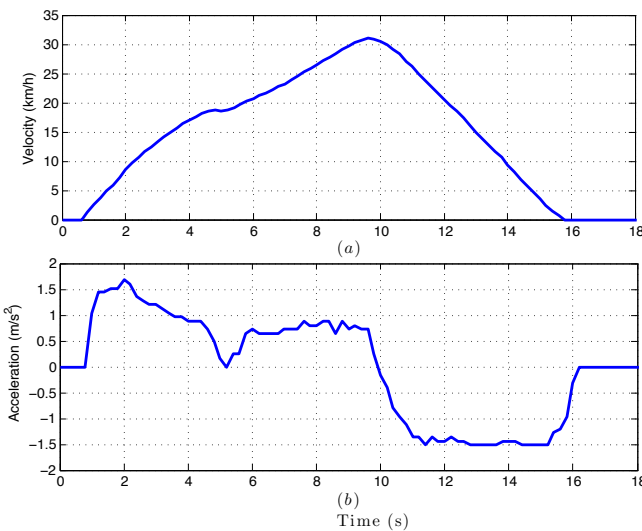


Fig. 6: Brake Control: (a) velocity, (b) acceleration

Fig. 7 (Experiment I) and 8 (Experiment II) show a comparison between simulation and experimental results of the

controlled vehicle for two different variable speed references. Velocity tracking, acceleration and normalized control action are shown in each figures. As it can be seen, the results show that the acceleration and control action are met the desired intervals. One can appreciate the soft action over vehicle's actuators obtaining a good comfort for car's occupants – this is reflected in the acceleration values. Moreover, the experimental results are tracked the reference value in both brake and throttle actions which is also verify the simulations results.

To sum up, fractional order hybrid controllers can be useful controllers to control autonomous vehicles in the brake and throttle action, specially due to its possibility of obtaining more adjustable time and frequency responses and allowing the fulfillment of more robust performances. The vehicle behavior is significantly good, especially concerning the comfort of vehicle's occupants.

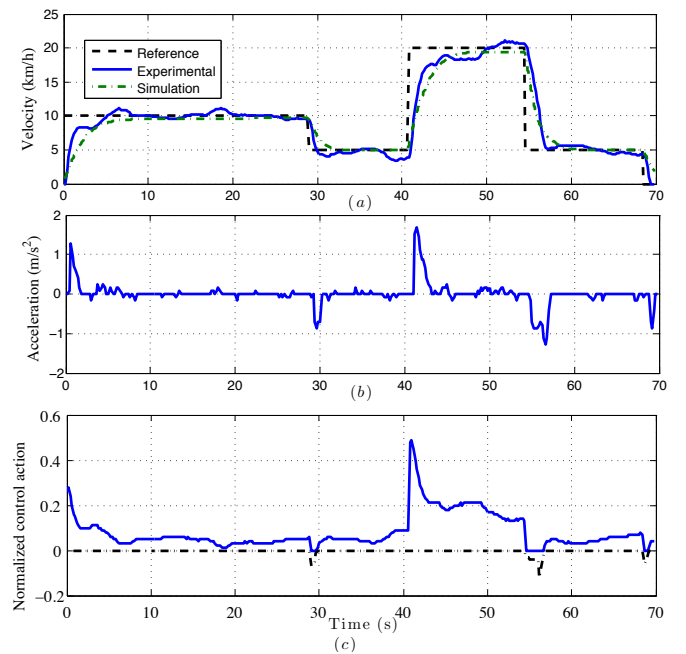


Fig. 7: Cruise control results for Experiment I: (a) velocity, (b) acceleration, (c) normalized control action

#### A. Digital implementation of fractional order controllers

It has to be taken into account that a fractional order controller is an infinite-dimensional linear filter, and that all existing implementation schemes are based on finite-dimensional approximations. In practice, we use a digital method, specifically the indirect discretization method, which requires two steps: firstly obtaining a finite-dimensional continuous approximation, and secondly discretizing the resulting  $s$ -transfer function. In our case, in order to preserve the integral effect, the integral part  $s^{-\alpha}$  has been implemented as follows:  $s^{-\alpha} = s^{-1}s^{1-\alpha}$ . Therefore, only the fractional part  $R_d(s) = s^{1-\alpha}$  has been approximated.

To obtain a finite-dimensional continuous approximation of the fractional order differentiator, the modified



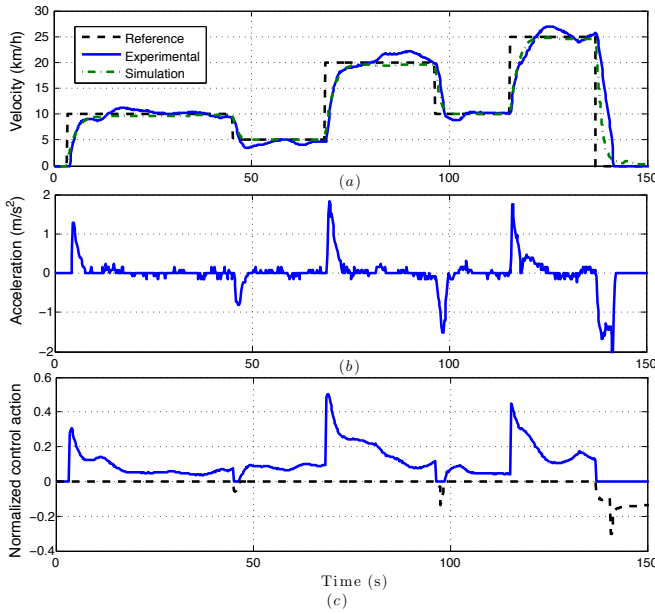


Fig. 8: Cruise control results for Experiment II: (a) velocity, (b) acceleration, (c) normalized control action

Oustaloup's method is used (see e.g. [3]). Thus, an integer order transfer function that fits the frequency response of  $R_d(s)$  in the range  $\omega \in (10^{-3}, 10^3)$  is obtained with 7 poles and 7 zeros. Later, the discretization of this continuous approximation is carried out by using the Tustin rule with a sampling period  $T_s = 0.2s$  -GPS sampling period-, obtaining the following digital IIR filters:

- Throttle controller:

$$R_{dT}(z) = \frac{\sum_{k=0}^7 b_k z^{-k}}{1 + \sum_{k=1}^7 a_k z^{-k}}, \quad (24)$$

where  $b_0 = 0.1573$ ,  $b_1 = 0.1325$ ,  $b_2 = -0.4389$ ,  $b_3 = -0.3658$ ,  $b_4 = 0.406$ ,  $b_5 = 0.3342$ ,  $b_6 = -0.1244$ ,  $b_7 = -0.1009$ ,  $a_1 = -0.8662$ ,  $a_2 = -2.746$ ,  $a_3 = 2.339$ ,  $a_4 = 2.507$ ,  $a_5 = -2.095$ ,  $a_6 = -0.7602$  and  $a_7 = 0.6211$ . Therefore, the resulting total fractional order controller is an 8th-order digital IIR filter given by:

$$C_T(z) = 0.09 + 0.025 \left( \frac{1-z^{-1}}{T_s} \right) R_{dT}(z).$$

- Brake controller.- The fractional part of this controller  $R_{dB}(z)$  was implemented by (24) but with the following coefficients:  $b_0 = 0.3529$ ,  $b_1 = 0.1878$ ,  $b_2 = -1.0274$ ,  $b_3 = -0.5381$ ,  $b_4 = 0.9959$ ,  $b_5 = 0.5128$ ,  $b_6 = -0.3215$ ,  $b_7 = -0.1625$ ,  $a_1 = -0.5400$ ,  $a_2 = -2.88062$ ,  $a_3 = 1.5053$ ,  $a_4 = 2.7658$ ,  $a_5 = -1.3952$ ,  $a_6 = -0.8852$  and  $a_7 = 0.4299$ . In this case, the resulting total fractional order controller is an 8th-order digital IIR filter given by:

$$C_B(z) = 0.07 + 0.11 \left( \frac{1-z^{-1}}{T_s} \right) R_{dB}(z).$$

## V. CONCLUSION

A hybrid fractional order controller is proposed to control the velocity of the car in low speed. The system is modeled as a hybrid differential inclusions. The system has different dynamics during the acceleration and deceleration of the car, and therefore different controllers are needed. A fractional order PI is used to control the throttle action, whereas a robust fractional order PI controller is designed for the uncertain model identified regarding to different brake actions. Both simulated and experimental results show the efficiency of the proposed strategy.

## REFERENCES

- [1] V. Milanés, J. Villagrà, J. Godoy, and C. González, "Comparing Fuzzy and Intelligent PI Controllers in Stop-and-Go Manoeuvres," *IEEE Transactions on Control Systems Technology*, doi:10.1109/TCST.2011.2135859, 2011.
- [2] J. Plà, "An Initiative of the Idea in Favour of Energy Efficiency in Transport.," Technical Report, Industry Department, 2009.
- [3] C.A. Monje, Y.Q. Chen, B.M. Vinagre, D. Xue, and V. Feliu, "Fractional-order Systems and Controls. Fundamentals and Applications," *Springer*, 2010.
- [4] Y.Q. Chen, I. Petras, and D. Xue, "Fractional Order Control: A Tutorial", In: *Proceedings of the 2009 American Control Conference (ACC'09)*, pp. 1397-1411, 2009.
- [5] A. Oustaloup. *La Commade CRONE: Commande Robuste d'Ordre Non Entier*. Paris: Hermes, 1991.
- [6] I. Podlubny, "Fractional-Order Systems and  $PI^\lambda D^\mu$  Controllers," *IEEE Transactions on Automatic Control*, vol. 44, pp. 208–214, 1999.
- [7] E. Onieva, V. Milanés, C. González, T. de Pedro, J. Pérez, J. Alonso, "Throttle and Brake Pedals Automation for Populated Areas," *Robotica*, vol. 28, pp. 509–516, 2010.
- [8] V. Milanés, D. Llorca, B. Vinagre, C. Gonzalez, and M. Sotelo, "Clavileño: Evolution of an autonomous car," in *Proc. of 13th International IEEE Conference on Intelligent Transportation Systems*, 2010.
- [9] I. Tejado, V. Milanés, J. Villagrà, J. Godoy, H. HosseinNia and B. M. Vinagre, "Low Speed Control of an Autonomous Vehicle by Using a Fractional PI Controller, IFAC world congress, 2011.
- [10] A. RodríguezCastaño, Estimación de Posición y Control de Vehículos Autónomos a Elevada Velocidad. *PhD Thesis*, University of Sevilla, Spain, 2007.
- [11] A. Kamga, and A. Rachid, Speed, Steering Angle and Path Tracking Controls for a Tricycle Robot. In: *Proceedings of the 1996 IEEE International Symposium on Computer-Aided Control System Design*, pp. 56-61, 1996.
- [12] V. Milanés, C. González, J. Naranjo, E. Onieva, and T. De Pedro, "Electro-hydraulic braking system for autonomous vehicles," *International Journal of Automotive Technology*, vol. 1, no. 11, pp. 8995, 2010.
- [13] C. A. Monje, B. M. Vinagre, Y.Q. Chen, V. Feliu, "On Fractional  $PI^\lambda$  Controllers: Some Tuning Rules for Robustness to Plant Uncertainties," *Nonlinear Dynamics*, vol. 38, no. (1-4), pp. 369-381, 2003.
- [14] J. Villagrà, V. Milanés, J. Pérez, and T. de Pedro, "Control Basado en PID Inteligentes: Aplicación al Control de Crucero de un Vehículo a Bajas Velocidades," *Revista Iberoamericana de Automática e Informática Industrial*, vol. 7, no 4, pp. 44–52, 2010.
- [15] V. Milanés, J. E. Naranjo, C. Gonzalez, J. Alonso, and T. de Pedro, "Autonomous vehicle based in cooperative gps and inertial systems," *Robotica*, vol. 26, pp. 627633, 2008.